J Mater Sci (2008) 43:3938–3945
DOI 10.1007/s10853-007-2334-y

Thermal reaction of SiC films with tungsten and tungsten–rhenium alloys

Jérome Roger · Fabienne Audubert · Yann Le Petitcorps

Received: 16 July 2007 / Accepted: 19 November 2007 / Published online: 13 March 2008
© Springer Science+Business Media, LLC 2008

Abstract Solid-state reactions between SiC films and W–xRe ($x = 0$, 5 and 25 at%) substrates on thermal annealing between 1673 K and 1873 K for various durations have been investigated. SiC coatings were deposited on metallic wires by hot filament chemical vapour deposition (HFCVD) from a gas mixture of tetramethylsilane (TMS) and hydrogen at 1373 K under normal pressure. The interface zones were characterized using scanning electron and optical microscopies, X-ray diffraction and electron microprobe microanalysis. All analyses reveal that SiC reacts with substrates. Various metal silicides and carbides were formed in layered reaction and the presence of these phases was confirmed by electron probe microanalysis. The effects of rhenium on the reactivity were established by the determination of growth kinetics deducted from the thicknesses of reaction zones as a function of annealing time. It has been found that an increase in the diffusion kinetics and activation energy with the quantity of rhenium in the tungsten wire.

Introduction

Silicon carbide is a very promising material for many applications at high temperatures, e.g. coating for nuclear fuel particles, ceramic matrix composites for engines or space shuttle structure components and high power electronic devices. SiC has numerous advantages including high melting point, low density, good mechanical behaviour, large energy gap, resistance to oxidation at high temperatures and chemical inertness to corrosive media [1–5]. The possibility of the occurrence of interface reactions between the silicon carbide and metals may lead to chemical instabilities and to a consequent deterioration of the properties. It is evident that there is a substantial interest in understanding reaction mechanisms of SiC with metals. Many articles have previously examined the thermal compatibility issues between SiC and transition metals [6–10]. Particularly, the interface reaction between SiC and W was previously studied between 873 K and 1373 K and revealed the existence of a reaction with formation of a silicide and a carbide [11, 12]. It is of particular interest to determine a solution to reduce this interface reaction. A way to limit the reactivity of W with SiC could be the addition of a few percent of another metal less reactive. Considering that on one side no rhenium carbide has been reported [13] and on the other side rhenium metal does not react with SiC [14], this metal could be an interesting alloy element to reduce the interfacial reaction with SiC. Moreover, rhenium forms a solid solution with tungsten up to 25 at% of Re at low temperature, this quantity can increase with temperature [15]. The diffusion coefficients of carbon in tungsten and tungsten–rhenium alloys were determined early at high temperature but only for low rhenium-containing samples (3.9 and 6.8 at% Re) [16, 17]. It remains an unknown parameter concerning the reactivity kinetic of rhenium with silicon atoms particularly in presence of tungsten.

The purpose of this study was to investigate the temperature stability of SiC films deposited on tungsten and

J. Roger (✉) · Y. Le Petitcorps
Université Bordeaux 1, Laboratoire des Composites Thermostructuraux, UMR 5801 (CNRS-SAFRAN-CEA-UB1), 3 Allée de la Boétie, 33600 Pessac, France
e-mail: roger@lcts.u-bordeaux1.fr

J. Roger · F. Audubert
Commissariat à l'Energie Atomique, DEN/DEC/SPUA/LTEC, Cadarache, 13108 Saint-Paul-Lez-Durance, France

tungsten–rhenium (5 and 25 at% Re) substrates at elevated temperatures of 1673, 1773 and 1873 K for various annealing durations. The resulting metal-SiC reactions were investigated with the help of several analysis techniques to determine the reaction zone dimensions in relation to annealing time and temperature. From these data, growth kinetics on the three substrates (W, W–5Re, W–25Re) for each temperature and the corresponding activation energies were calculated.

Experimental methods

For this study, the diffusion couples were prepared by the chemical vapour deposition of SiC on 100 μm diameter wire substrates of pure W (99.95% purity) and W–*x*Re with $x = 5$, 25 at% of Re (99.9% purity) supplied by Googfellow company, the low temperature limit of this solid solution being 25 at% of Re [15]. SiC layers growth was carried out in a cold-wall reactor by Chemical Vapour Deposition (CVD) from tetramethylsilane (TMS) as precursor in presence of hydrogen as the dilution and reducing gas. TMS was used as a source gas containing both silicon and carbon atoms, this precursor which decomposes at 1073 K is well known to form quasi-stoichiometric β-SiC layers [18]. During deposition, the metallic wire substrates were then resistively heated at 1373 K as measured by an optical pyrometer. After 6 min, the SiC thickness was of about 20 μm which was considered sufficient for our study. The deposition experiments were performed under normal pressure at constant flows of TMS (10 sccm) and H_2 (150 sccm). Prior to the SiC growth, the substrates were thermally treated at 1273 K for 10 min in 250 sccm pure H_2 flow to eliminate innate impurities. A titanium wire heated at 1500 K for 10 min was also used as an oxygen getter.

In order to establish the reactivity at high temperature of the metallic alloys with the SiC, the samples were treated at three various temperatures and times. The samples introduce into a graphite crucible were then annealed with the help of a high frequency furnace for the shortest treatments in time or a tube furnace for the longest ones, both flushed with Ar. After annealing, metal/SiC couples were investigated using a X-ray diffractometer (XRD, Siemens D5000) using a Cu Kα radiation to identify the formed phases and a scanning electron microscope (SEM, JEOL JSM 6360A) to observe the sample morphologies. In order to profile the atomic composition, the reaction zones were also analysed on polished section with an electron probe microanalyzer (EPMA, Cameca SX-100) with wavelength-dispersive spectrometer operated at an acceleration voltage of 20 kV, and a probe size of 1 μm in diameter. It is worth noting that the detection of carbon was quite difficult owing to the Au sputtering, that is why for those analyses, carbon concentrations were determined by difference. The thickness of the reaction zones was measured with an optical microscope. At least 10 measurements were taken, and then the mean thickness was calculated. For those analyses, the annealing couples were embedded in epoxy resin and polished with diamond suspension down to 1 μm in size.

Results and discussion

Characterization of the W–*x*Re/SiC diffusion couples

The X-ray diffraction pattern taken from the surface of the as-deposited coatings presented on Fig. 1 shows clearly the crystallization of textured β-SiC, indeed the intensities of (200) and (220) reflections are stronger than those reported for the SiC standard. EPMA micro-analysis revealed that SiC is practically stoichiometric. The presence of a few quantity of free carbon is established but does not affect the results.

The following characterizations were realized on the samples annealed at 1773 K for 5 h since the reaction zones were sufficiently developed to be examined and at the sametime, the substrates were not fully consumed. Figure 2 shows the optical micrographies of the W–*x*Re/SiC diffusion couple with $x = 0$, 5 and 25 at% of Re. In each case, reaction layers are visible and exhibit a typical columnar morphology concentric to the centre of the substrate. The Kirkendall voids observed at the interface between SiC and the reaction zone indicate a diffusion rate more elevated for Si and C than for metal atoms. Those observations are confirmed by the secondary electron and BackScattered Electron (BSE) images presented on Figs. 3 and 4. From the BSE images (Fig. 4b, d, f), the number of the grown phases can be easily deducted, thus the formation of the two phases is observed for the samples on pure W and W–5Re. In the case of the sample with W–25Re, the corresponding BSE image reveals the presence of four

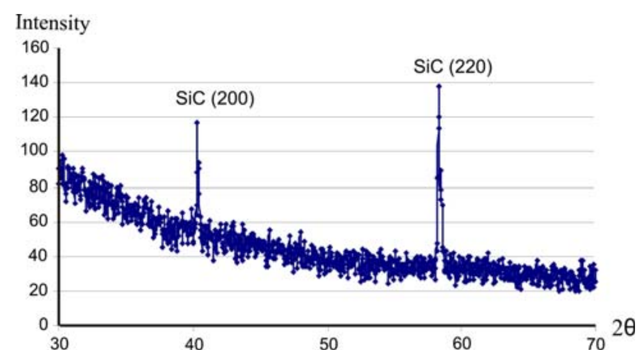

Fig. 1 X-ray diffraction pattern measured on the surface of W/SiC diffusion couple before annealing

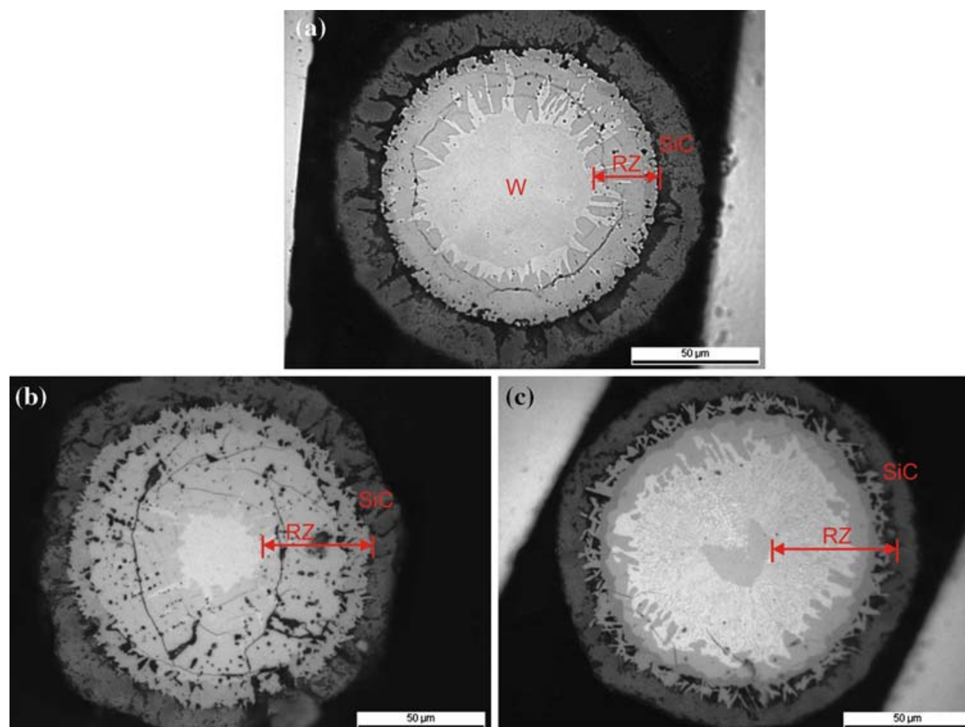

Fig. 2 Optical images of the W–xRe/SiC diffusion couple annealed at 1773 K for 5 h: (**a**) $x = 0$, (**b**) $x = 5$ and (**c**) $x = 25$ at% of Re

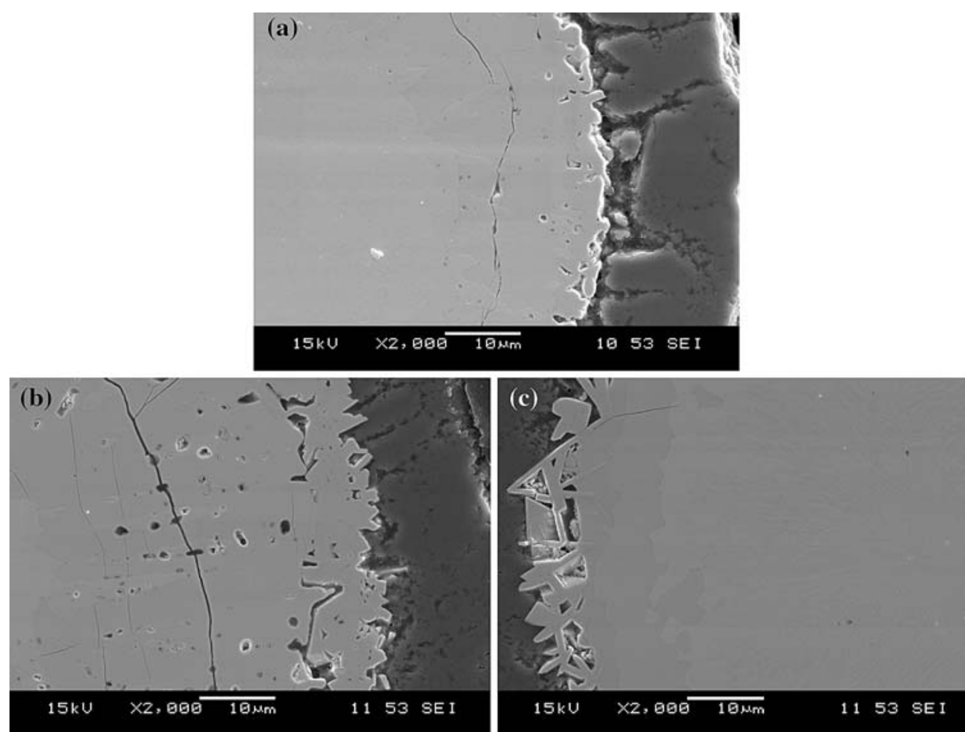

Fig. 3 Secondary electron images of the cross-section of the W–xRe/SiC diffusion couples heat-treated at 1773 K for 5 h: (**a**) $x = 0$, (**b**) $x = 5$ and (**c**) $x = 25$ at% of Re

zones: from the board to the centre of the wire, we notice the formation of a needle-like grown phase partially occupying the Kirkendall voids, two others concentric phases are then detected. The last zone is made of dendrites indicating a segregation mechanism. The samples exhibit many cracks; some of them have been formed during cooling from the annealing temperature to room temperature, the existence of these defaults is induced by the mismatch of the thermal expansion coefficients between the reaction layer and the substrate (Figs. 3, 4).

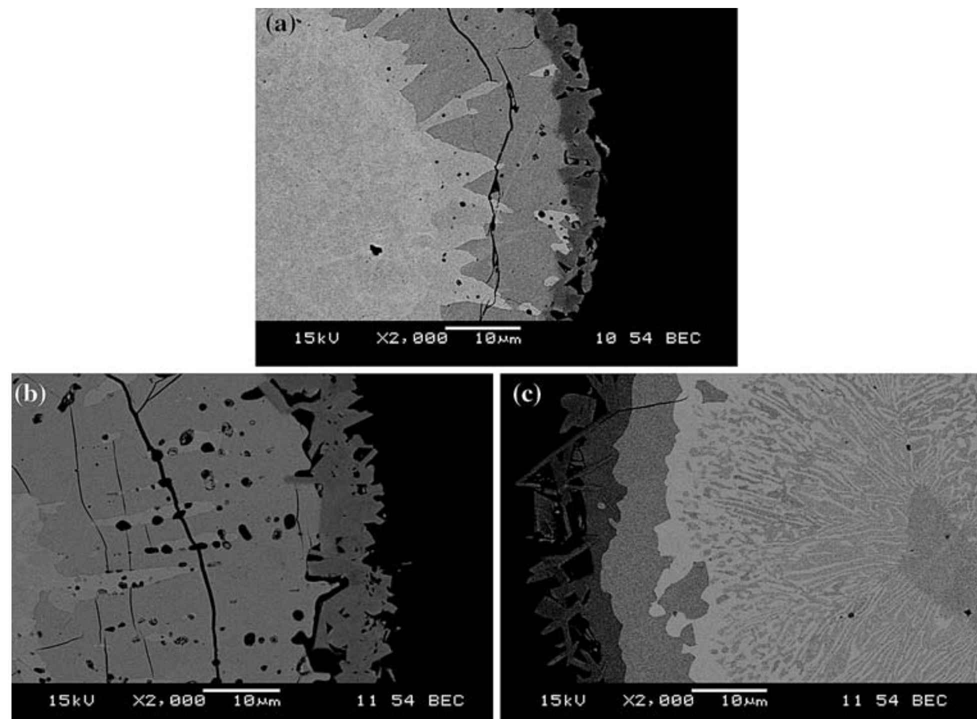

Fig. 4 Backscattered electron images of the cross-section of the W/SiC diffusion couples heat-treated at 1773 K for 5 h: (**a**) $x = 0$, (**b**) $x = 5$ and (**c**) $x = 25$ at% of Re

X-ray diffraction powder patterns were realized for each annealed sample to investigate the phases formed during the diffusion mechanism. The diffraction patterns revealed for each couple the presence of unreacted SiC and the formation of WC and W_5Si_3 related phases (Fig. 5). In the case of the W–25Re substrate containing sample, one additional phase is detected but remains unidentified up to now.

W/SiC diffusion couple

On the Fig. 6 are presented the concentration profiles got though the diameter of the samples heat treated at 1773 K for 5 h with an interval of 1 μm. Particularly, Fig. 6a concerns the W/SiC couple and shows the experimental concentration profiles of tungsten, silicon and carbon, concentration of this last element being deducted by difference. According to X-ray measurements, the phases detected are WC with some traces of Si (W:C:Si = 49.9:48.3:2.9 at%) and a phase derivative from W_5Si_3 containing some traces of C (W:Si:C = 62.6:35.9:1.9 at%). The width reaction zone of this silicide noted $W_5Si_3C_\varepsilon$ (18 μm) is quite more extended than the corresponding one of the carbide (4 μm). From the results obtained during our own study, the diffusion path for the couple W/SiC between 1673 and 1873 K can be deduced and is plotted in Fig. 7. Our observations agree well with the conclusions proposed by Goesmann and Schmid-Fetzer [1].

W–5Re/SiC diffusion couple

In agreement with the phases identified on X-ray diffraction pattern of the W–5Re substrate sample, the WDS concentration profiles reveal the formation of a phase noted (W, Re) C with some traces of forwarding Si, this phase is connected to WC with the following atomic composition W:Re:Si:C = 48:1:2:49. The second formed phase is clearly derivative of W_5Si_3, the mean atomic composition indicates a partial substitution of W by Re atoms (W:Re:Si:C = 60:3:31:6 at%). Measurements realized on the unreacted substrate lead to a tungsten/rhenium ration equal to 96/4 in good agreement with the composition announced by the supplier considering an error of about 1 atomic percent.

W–25Re/SiC diffusion couple

The analysis realized on the W–25Re/SiC diffusion couple annealed at 1773 K for 5 h revealed a chemical reactivity more complex than for the two previous samples. For more comprehension, weight concentration cartographies on a

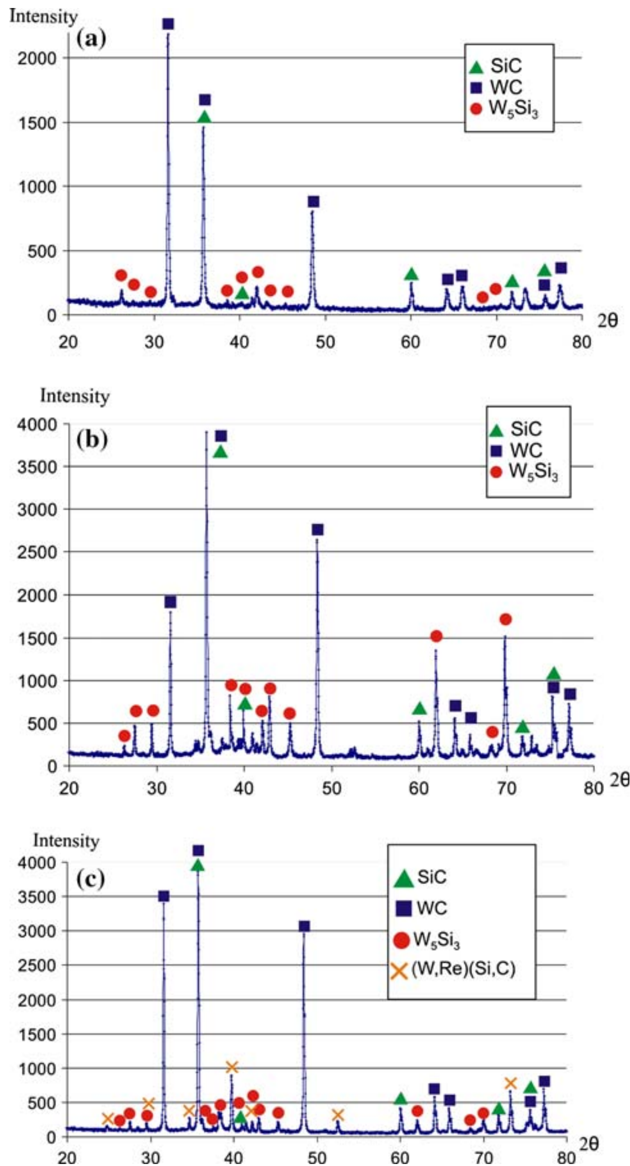

Fig. 5 X-ray powder diffraction patterns measured on the W–*x*Re/SiC diffusion couples annealed at 1773 K for 5 h crushed in powder: (**a**) $x = 0$, (**b**) $x = 5$ and (**c**) $x = 25$ at% of Re

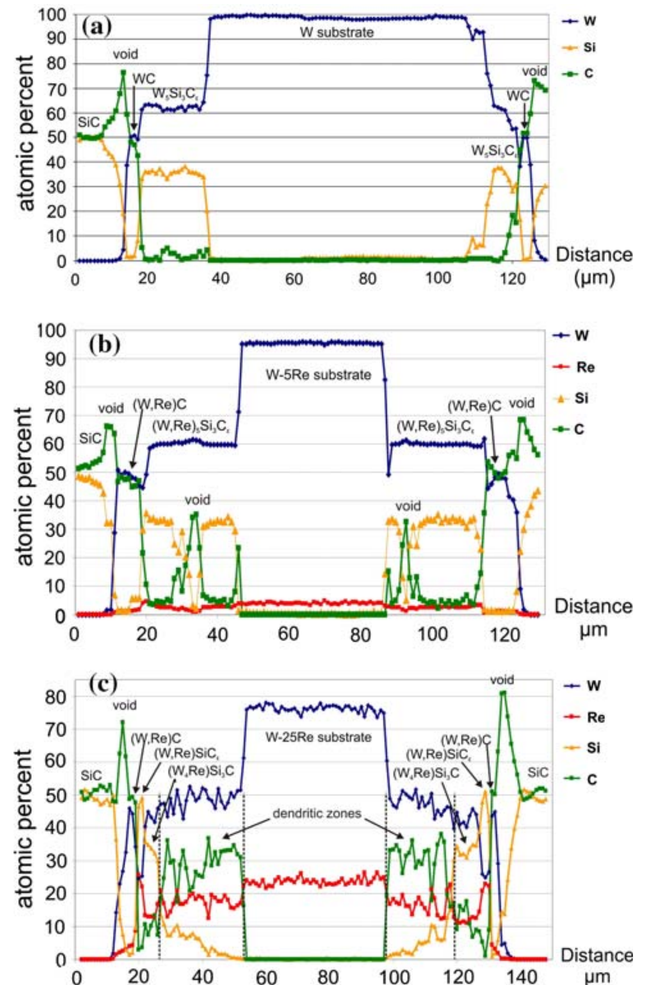

Fig. 6 WDS experimental concentration profiles of tungsten, rhenium, silicon and carbon by EPMA measured on the diameter of the W–*x*Re/SiC diffusion couples annealed at 1773 K for 5 h: (**a**) $x = 0$, (**b**) $x = 5$ and (**c**) $x = 25$ at% of Re. Carbon concentration is determined by difference. On (**c**), dendritic zones are delimited by dashed lines

selected region of this couple were realized for W, Re and Si, results are presented in Fig. 8.

From the weight concentration cartographies and the corresponding WDS concentration profiles for W, Re and Si, it appears that four different zones are formed, according to the observations realized on optical images. From the SiC side to the centre of the wire, we find first a phase connected to WC with a quantity quite higher than on W–5Re substrate, we also find some traces of silicon (W:Re:C:Si = 45:4:50:1 at%). The atomic ratio of the second phase has been found equal to W:Re:C:Si = 25:23:49:3. This unidentified phase is very rich in rhenium and silicon as highlighted on the Re and Si concentration cartographies (Fig. 8c, d). The following phase is much more extended and presents the atomic composition W:Re:Si:C = 60:3:31:6 which agrees well with the metal/metalloid ratio of the W_5Si_3 phase. The phase in question is obviously derivative from the silicide with partial substitution of W and Si by Re and C atoms, respectively. The fourth zone, as previously mentioned, is made of dendrites; the corresponding concentration profiles indicate the presence of the four elements with important fluctuations. As shown in the Fig. 8b, c, this zone is composed of two different phases, the first one is richer in rhenium and silicon than the second one. The mean composition calculated on the basis of five points measured on the sample annealed at 1873 K for 8 h revealed that this phase has atomic

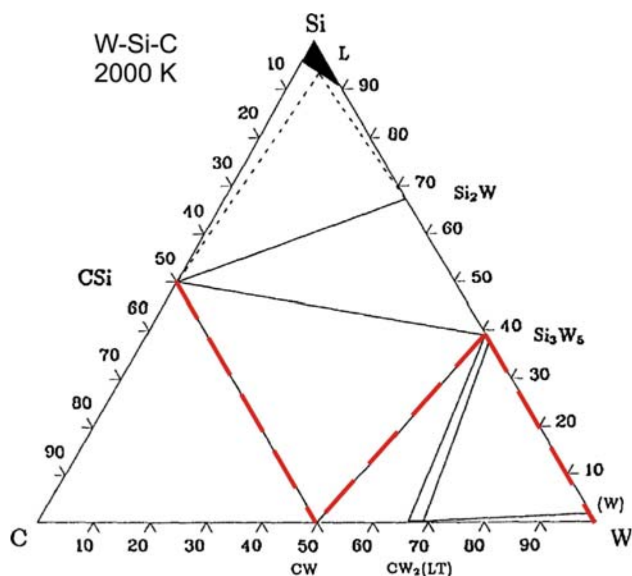

Fig. 7 Isothermal section of the W–Si–C phase diagram at 2000 K. The diffusion path for the couple W/SiC is indicated by the dashed thick red lines

composition W:Re:Si:C = 40:25:15:20. In fact, this quaternary compound presents a W/Re ratio very low comparing to the substrate composition, it can be concluded that the formation of this compound induces a faster consumption of rhenium atoms leading to a Re concentration decrease of the metallic substrate. In consequence, two phases coexist; the first one corresponding to the quaternary compound, the second one being the W–Re alloy with a composition gradient observable in Fig. 8c. The tungsten/rhenium ratio of the unreacted substrate was found equal to 76/24, in good agreement with the composition announced by the supplier.

Growth kinetics

Figure 9 is a plot of the thicknesses of the reaction zones for the three kinds of substrates versus the square root of annealing time between 1673 and 1873 K. In each case, the reaction kinetic obeys a parabolic kinetics law. It is worth noting that those curves are obtained after applying a mathematical correction in order to transform the cylindrical geometry into an equivalent planar one geometry. This correction considers that the diffused volume is constant, which induces an error in the case of a non-planar geometry, especially when the reaction zone is extended and/or the wire radius is small. Practically, we calculated

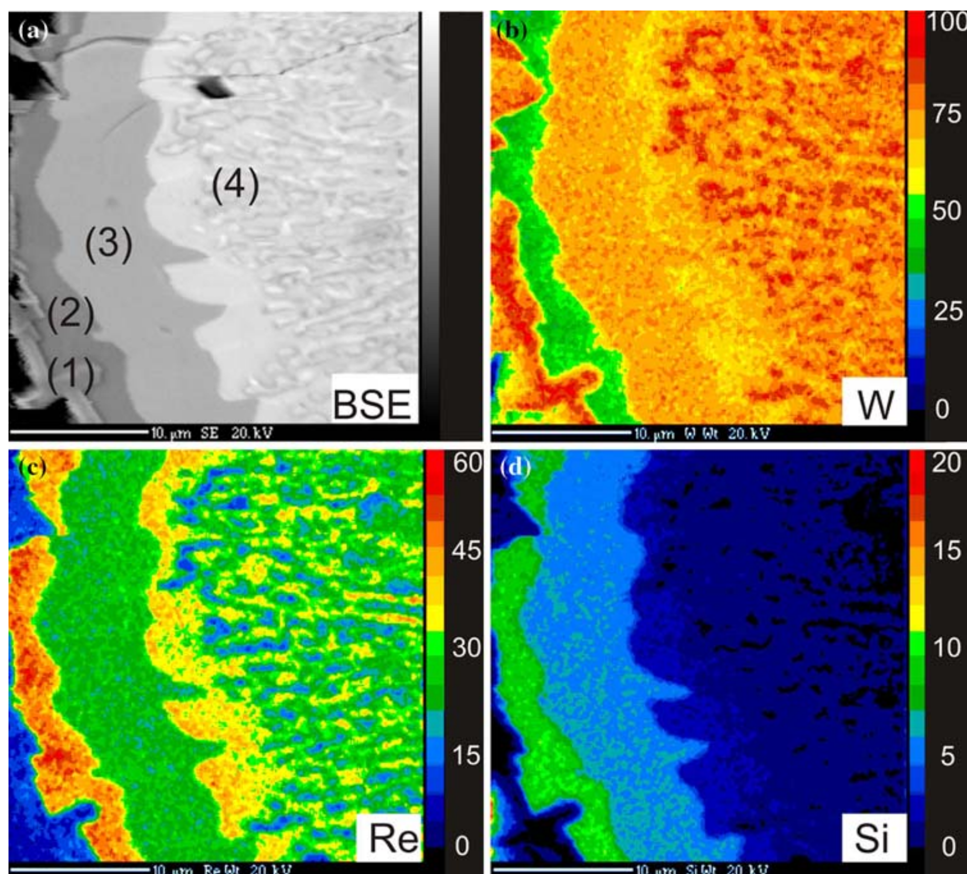

Fig. 8 Detail analyses of the W–25Re/SiC diffusion couple heat treated at 1773 K for 5 h: (**a**) backscattered electron image, weight concentration cartographies of (**b**) W, (**c**) Re and (**d**) Si

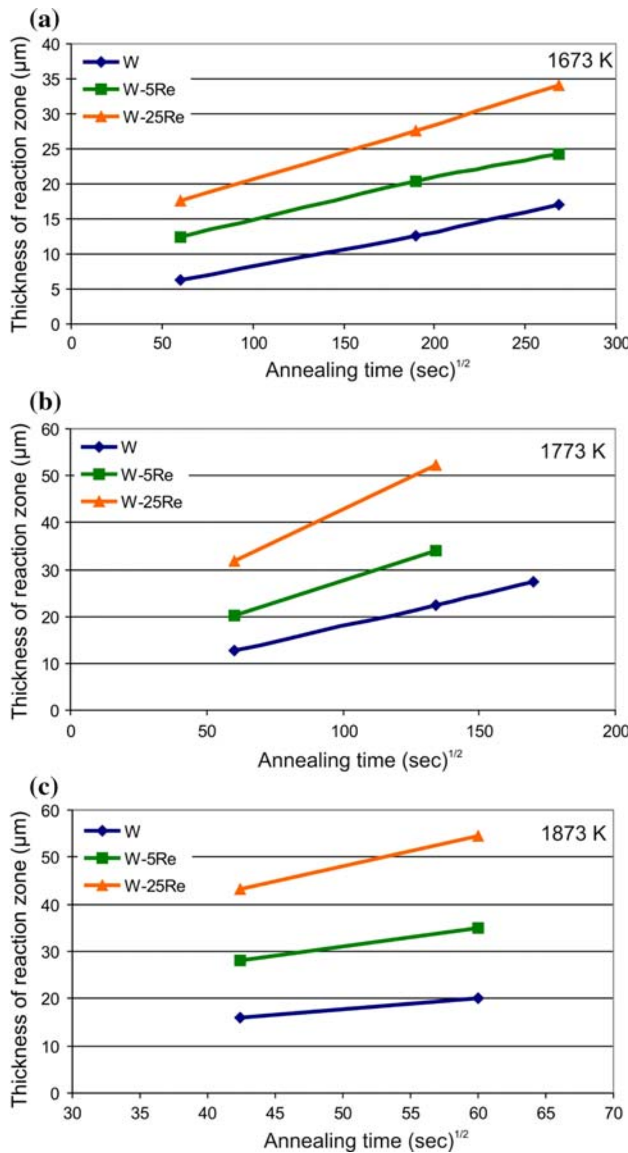

Fig. 9 Linear regression fit of the plots of the thicknesses of the diffusion zones grown by annealing of W–*x*Re/SiC ($x = 0$, 5 and 25 at%) diffusion couples versus the square root of annealing time: (**a**) 1673 K, (**b**) 1773 K and (**c**) 1873 K

the surface of the reaction zone and determined the corresponding reaction zone thickness on an equivalent planar substrate of $2\pi R$ width, R being equal to 50 µm in the present case. Another correction has to be applied considering that the extrapolated curves of the thicknesses do not pass through the origin. The thickness (x_0) of the reaction zone at zero time differ from 0, those shifts are induced by the growth reactions that already occur during the coating by CVD and the heating and cooling stages of annealing treatments. In order to evaluate the growth rate constant, the data were fitted according to the modified Eq. 1:

$$(x - x_0)^2 = 2k_p \cdot t \quad (1)$$

where x and k_p are respectively the thickness and parabolic growth rate constant of reaction layer and t is the annealing time. The parabolic growth rate constants for each temperature and substrate can be easily deducted from the slope of the corresponding curves. From the shape of those curves, it can be concluded that the reaction zone thicknesses are functions of Re concentration. It appears richer in the initial substrate in rhenium, faster in the diffusion reaction.

Figure 10 is a plot of the linear relationship of the logarithm of k_p versus the reciprocal of the absolute temperature T. The curves follow an Arrhenius relationship $k_p = k_0 \exp(-Q/RT)$, where k_0 is the frequency factor and Q the apparent activation energy of the interface reaction between SiC and the metallic substrate. The addition of rhenium into the substrate induces an increase of the activation energy while the values of Q were calculated to be about 98, 121 and 131 kcal mol^{-1} on W, W–5Re and W–25Re substrates, respectively. When comparing the value obtained on W with previous studies realized by Lee et al. [19] on growth kinetic of W_5Si_3 in WSi_2/W system, it appears that the activation energy equal to 88 kcal mol^{-1} is somewhat lower than our value on W. This difference is relative to the higher stability of SiC comparing to silicides. Contrary to the conclusions proposed by Shepela [16] about the diffusion of carbon in W and W–*x*Re alloys, our study concerning the W–*x*Re/SiC system reveals that the activation energy and growth rate increase with increasing rhenium content. This finding is somewhat surprising since a previous study realized by Chen et al. [14] indicated that no reaction occurs between SiC and Re.

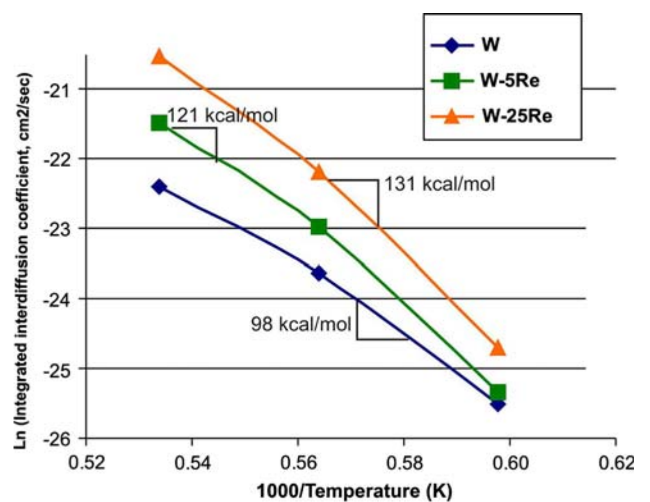

Fig. 10 Arrhenius plots of the parabolic rate constants of the diffusion zones grown by annealing of W–*x*Re/SiC ($x = 0$, 5 and 25 at%) diffusion couples as a function of the reciprocal absolute temperature

Conclusion

The SiC films were deposited on W–xRe ($x = 0$, 5 and 25 at%) wires by hot filament chemical vapour deposition at 1373 K from TMS. After annealing between 1673 K and 1873 K, all samples react with formation of WC and W_5Si_3 derivative phases. In the particular case of the richest Re containing sample, two other unidentified phases also appear with the formation of a dendritic zone. The study of the growth rate constants and activation energies reveals an increase of those values with rhenium content. In consequence, this metal cannot be used as a reaction limiter. The chemical mechanism leading to an increase of reactivity of W in presence of Re is not precisely determined at the present time. Nevertheless, the origin of this increase is probably in link with the disorder induced by the addition of rhenium atoms. The presence of those atoms could lead to a thermal activation of microscopic mobility in relation with modifications of energy levels. Further experimental investigations on the W–xRe/SiC couple seem necessary to settle this point.

Acknowledgements The authors wish to thank M. Lahaye (CeCaMA, Bordeaux) for his assistance in SEM and EPMA studies.

References

1. Goesmann F, Schmid-Fetzer R (1995) Mater Sci Eng B34:224
2. Space RI, Slack GA (1960) In: O'Connor JR, Smiltens J (eds) Silicon carbide, a high-temperature semiconductor. Pergamon, New York
3. Ryan CE (1969) Mater Res Bull S1:4
4. Price RJ (1977) Nucl Technol 320:35
5. Sasaki K, Sakuma E, Misawa S, Yoshida S, Gonda S (1984) Appl Phys Lett 72:45
6. Geib KM, Wilson C, Long RG, Wilmsen W (1990) J Appl Phys 68:2796
7. Tang WM, Zheng ZX, Ding HF, Jin ZH (2003) Mater Chem Phys 80:360
8. Bhanumurthy K, Schmid-Fetzer R (2001) Composites 32A:569
9. Chou TC, Joshi A, Wadsworth J (1991) J Mater Res 6(4):796
10. van Loo FJJ, Smet FM, Rieck GD, Verspui G (1982) High Temp High Pres 14:25
11. Brewer L, Krikorian O (1956) J Electrochem Soc 103:38
12. Baud L, Jaussaud C, Madar R, Bernard C, Chen JS, Nicolet MA (1995) Mater Sci Eng B29:126
13. Searcy AW, Finnie LN (1962) J Am Ceram Soc 45(6):268
14. Chen JS, Kolawa E, Nicolet M-A, Baud L, Jaussaud C, Madar R, Bernard C (1994) J Appl Phys 75(2):897
15. Liu Z-K, Austin Chang Y (2000) J Alloys Compds 299:153
16. Shepela A (1972) J Less-Common Met 26:33
17. Schmid K, Roth J (2002) J Nuclear Mater 302:96
18. Henry F, Armas B, Combescure C, Figueras A, Garelik S (1996) Surf Coat Tech 90:134
19. Lee K-H, Yoon J-K, Lee J-K, Doh J-M, Hong K-T, Yoon W-Y (2004) Surf Coat Tech 187:146